QUADRATIC DIFFERENTIAL SYSTEMS WITH A FINITE SADDLE–NODE AND AN INFINITE SADDLE–NODE $(1,1)SN$ - (A)

JOAN C. ARTÉS
Departament de Matemàtiques, Universitat Autònoma de Barcelona, 08193 Bellaterra, Barcelona, Spain
E–mail: artes@mat.uab.cat

MARCOS C. MOTA
Instituto de Ciências Matemáticas e de Computação, Universidade de São Paulo, 13566–590, São Carlos, São Paulo, Brazil,
E–mail: coutinhomotam@gmail.com

ALEX C. REZENDE
Departamento de Matemática, Universidade Federal de São Carlos, 13565–905, São Carlos, São Paulo, Brazil,
E–mail: alexcr@ufscar.br

Our goal is to make a global study of the class $\mathbf{QsnSN_{11}}$ of all real quadratic polynomial differential systems which have a finite semi–elemental saddle–node and an infinite saddle–node formed by the coalescence of a finite and an infinite singularities. This class can be divided into two different families, being (A) possessing the finite saddle–node as the only finite singularity and (B) possessing the finite saddle–node and also a finite simple elemental singularity. In this paper we provide the complete study of the geometry of family (A). The family (A) modulo the action of the affine group and time homotheties is four–dimensional and we give the bifurcation diagram of its closure with respect to a specific normal form, in the four–dimensional real projective space $\mathbb{RP}^4$. As far as we know, this is the first time that a complete family is studied in the four–dimensional real projective space. The respective bifurcation diagram yields 36 topologically distinct phase portraits for systems in the closure $\overline{\mathbf{QsnSN_{11}(A)}}$ within the representatives of $\mathbf{QsnSN_{11}(A)}$ given by a specific normal form.
Keywords: Quadratic differential systems; finite saddle–node; infinite saddle–node; phase portraits; bifurcation diagram; algebraic invariants.

1. Introduction, brief review of the literature and statement of the results

Here we call *quadratic differential systems*, or simply *quadratic systems*, differential systems of the form

$$\begin{array}{rcl} \dot{x} & = & p(x,y), \\ \dot{y} & = & q(x,y), \end{array} \tag{1}$$

where p and q are polynomials over $\mathbb{R}$ in x and y such that the $\max\{\deg(p), \deg(q)\} = 2$. To such a system one can always associate the quadratic vector field

$$\xi = p\frac{\partial}{\partial x} + q\frac{\partial}{\partial y}, \tag{2}$$

as well as the differential equation

$$q\,dx - p\,dy = 0. \tag{3}$$

Along this paper we will use indistinctly the expressions *quadratic systems* and *quadratic vector fields* to refer to either (1), or (2), or (3).

The class of all quadratic differential systems will be denoted by **QS**.

We can also write system (1) as

$$\begin{array}{rcl} \dot{x} & = & p_0 + p_1(x,y) + p_2(x,y) \equiv p(x,y), \\ \dot{y} & = & q_0 + q_1(x,y) + q_2(x,y) \equiv q(x,y), \end{array} \tag{4}$$

where p_i and q_i are homogeneous polynomials of degree i in the variables x and y with real coefficients and $p_2^2 + q_2^2 \neq 0$.

Even after hundreds of studies on the topology of real planar quadratic vector fields, it is kind of impossible to outline a complete characterization of their phase portraits, and attempting to topologically classify them, which occur rather often in applications, is quite a complex task. This family of systems depends on twelve parameters, but due to the action of the group $\mathrm{Aff}(2,\mathbb{R})$ of real affine transformations and time homotheties, the class ultimately depends on five parameters, but this is still a large number.

The main goal of this work is to present the study of the class of all quadratic systems possessing a finite saddle–node $\overline{sn}_{(2)}$ located at the origin of the plane and an infinite saddle–node of type $\binom{\overline{1}}{1} SN$. We denote this class by $\mathbf{QsnSN_{11}}$. We recall that a finite saddle–node is a semi–elemental singular point whose neighborhood is formed by the union of two hyperbolic sectors and one parabolic sector. By a semi–elemental singular point we mean a point with zero determinant of its Jacobian matrix with only one eigenvalue equal to zero. These points are known in classical literature as semi–elementary, but we use the term *semi–elemental* introduced in [Artés *et al.*, 2013a] as part of a set of new definitions more deeply related to singularities, their multiplicities and, especially, their Jacobian matrices. In addition, an infinite saddle–node of type $\binom{\overline{1}}{1} SN$ is obtained by the coalescence of a finite antisaddle (respectively, finite saddle) with an infinite saddle (respectively, infinite node).

Whenever one wants to study a specific family of differential systems sharing a common property, one needs to select one (or several) normal form which contains all the phase portraits sharing the desired property. However, except in some trivial cases, it is impossible that the normal form does not contain other phase portraits, normally more degenerate than the cases under study. These other phase portraits are very important to understand the bifurcations that take place inside the chosen normal form. This is why we always study not just the family of systems that have the desired property, but the closure of the normal form which contains that family. That is, we study all the parameter space of the selected normal form, whether if it leads to the desired property or not. However, it is possible that a different normal form could have been chosen and in that case, the generic elements of the family under study should be the same, but the elements in the border might not be. That is, some phase portraits in the border of one normal form could be common or not, with elements in the order of the second normal form.

Inside the class $\overline{\mathbf{QsnSN_{11}}}$ where generically the origin is a saddle–node $\overline{sn}_{(2)}$ and we have an infinite singularity of type $\binom{\overline{1}}{1} SN$, we may have or not another simple finite elemental singularity. Then, we split this class into two different families: $\mathbf{QsnSN_{11}(A)}$ of phase portraits possessing the finite saddle–node as the only finite singularity and $\mathbf{QsnSN_{11}(B)}$ of phase portraits possessing the finite saddle–node and also a simple finite elemental singularity. In this paper we provide the analysis of the closure of the family $\mathbf{QsnSN_{11}(A)}$.

We observe that there is another type of infinite saddle–node denoted by $\binom{\overline{0}}{2} SN$ which is given by the coalescence of an infinite saddle with an infinite node and which will appear in some of the phase

portraits obtained in the class $\overline{\mathbf{QsnSN_{11}(B)}}$. We point out that the family of quadratic differential systems possessing a finite saddle–node $\overline{sn}_{(2)}$ and an infinite singularity $\overline{\binom{0}{2}}SN$ was completely studied in [Artés *et al.*, 2015].

For this analysis we follow the pattern set out in [Artés *et al.*, 2015] and, in order to avoid repeating technical sections which are the same for both papers, we refer to the paper mentioned for more complete information.

We recall that all the phase portraits are drawn in the Poincaré disc (for its definition we refer to [Dumortier *et al.*, 2006, Artés *et al.*, 2015]) and in what follows we present the notion of *graphics*.

A *(nondegenerate) graphic* as defined in [Dumortier *et al.*, 1994] is formed by a finite sequence of singular points $r_1, r_2, \ldots, r_n$ (with possible repetitions) and nontrivial connecting orbits γ_i for $i = 1, \ldots, n$ such that γ_i has r_i as α–limit set and r_{i+1} as ω–limit set for $i < n$ and γ_n has r_n as α–limit set and r_1 as ω–limit set. Also normal orientations n_j of the nontrivial orbits must be coherent in the sense that if γ_{j-1} has left–hand orientation then so does γ_j. A *polycycle* is a graphic which has a Poincaré return map.

A *degenerate graphic* is formed by a finite sequence of singular points $r_1, r_2, \ldots, r_n$ (with possible repetitions) and nontrivial connecting orbits and/or segments of curves of singular points γ_i for $i = 1, \ldots, n$ such that γ_i has r_i as α–limit set and r_{i+1} as ω–limit set for $i < n$ and γ_n has r_n as α–limit set and r_1 as ω–limit set. Also normal orientations n_j of the nontrivial orbits must be coherent in the sense that if γ_{j-1} has left–hand orientation then so does γ_j. For more details, see [Dumortier *et al.*, 1994].

In [Artés *et al.*, 1998] the authors proved the existence of 44 topologically different phase portraits for the structurally stable quadratic planar systems modulo limit cycles, also known as the codimension–zero quadratic systems. Roughly speaking, these systems are characterized by having all singularities, finite and infinite, simple, no separatrix connection, and where any nest of limit cycles is considered as a single point with the stability of the outer limit cycle.

In the book of [Artés *et al.*, 2018] the authors classified the structurally unstable quadratic systems of codimension–one which have one and only one of the simplest structurally unstable objects: a saddle–node of multiplicity two (finite or infinite), a separatrix from one saddle point to another, and a separatrix forming a loop for a saddle point with its divergence nonzero. All the phase portraits of codimension–one are split into four groups according to the possession of a structurally unstable element: (A) possessing a finite semi–elemental saddle–node, (B) possessing an infinite semi–elemental saddle–node $\overline{\binom{0}{2}}SN$, (C) possessing an infinite semi–elemental saddle–node $\overline{\binom{1}{1}}SN$, and (D) possessing a separatrix connection. The study of the codimension–one systems was done in approximately 20 years and finally it was obtained at least 204 (and at most 211) topologically distinct phase portraits of codimension–one modulo limit cycles. However, some recent studies (already at preprint level) have shown two mistakes in that book and have reduced (and confirmed) the number of cases to 202 (and a most 209).

The next step is to study the structurally unstable quadratic systems of codimension two, modulo limit cycles. The approach is the same as used in the previous two works [Artés *et al.*, 1998, Artés *et al.*, 2018]. One must start by looking for all the topologically possible phase portraits of codimension two, and then try to realize all of them or show that some of them are impossible. So, it is also very convenient to have studied the bifurcation diagram that contains all the required phase portraits in order to prove the realization of them. In many works of this last type where families of phase portraits have been studied, it is quite common that the authors have missed one or several phase portraits, as we discuss in Sec. 2. This may happen either because they have not interpreted correctly some of the bifurcation parts, or they have missed the existence of some nonalgebraic bifurcation, or there may exist some small "island" as they are described in Sec. 7. However when one does the study of all the topological phase portraits and produces a list in a systematic way which is free of errors, then there is no possibility of missing a realizable case. It is just a problem of finding examples of realization or producing irrefutable proofs of the impossibility of realization of phase portraits.

The study of the codimension–two systems is already in progress. In [Artés *et al.*, 2019] the authors have considered the group (AA) obtained by

the existence of a cusp point, or two saddle–nodes or the coalescence of three finite singular points forming a semi–elemental singularity, yielding either a triple saddle, or a triple node. They obtained all the possible topological phase portraits of group (AA) and proved their realization. In their study, they got 34 topologically distinct phase portraits in the Poincaré disc modulo limit cycles.

Moreover, as we have already said, the bifurcation diagram for the class of the quadratic systems possessing a finite saddle–node $\overline{sn}_{(2)}$ and an infinite saddle–node $\binom{0}{2}SN$ has been studied in [Artés *et al.*, 2014, Artés *et al.*, 2015], in which all the phase portraits obtained belong to the closure of the group (AB).

The present study in this paper is part of this attempt of classifying all the codimension–two quadratic systems. All the phase portraits obtained in the study of the class $\overline{\mathbf{QsnSN_{11}(A)}}$ belong to the closure of the group (AC).

For the normal form (6) from page 8, the class $\overline{\mathbf{QsnSN_{11}(A)}}$ is partitioned into 75 parts: 11 four–dimensional ones, 21 three–dimensional ones, 24 two–dimensional ones, 14 one–dimensional ones and 5 points. This partition is obtained by considering all the bifurcation manifolds of singularities, one related to the presence of invariant straight lines and one related to connections of separatrices, modulo "islands" (see Sec. 7). Due to some values of the parameters, from these 75 parts, four of them correspond to linear systems, being two one–dimensional and two points (see page 22). The corresponding four phase portraits form two classes, as indicated in Fig. 1.

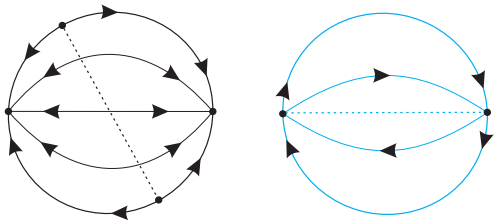

Fig. 1. Phase portraits corresponding to linear systems obtained from canonical form (6)

Theorem 1.1. *There are* 36 *topologically distinct phase portraits for the closure of the family of quadratic vector fields having a finite saddle–node* $\overline{sn}_{(2)}$ *as the only finite singularity and an infinite saddle–node of type* $\binom{1}{1}SN$*, and given by the normal form* (6) *(class* $\overline{\mathbf{QsnSN_{11}(A)}}$*). The bifurcation diagram for this class is given in the parameter space which is the projective four–dimensional space* $\mathbb{RP}^4$*. All these phase portraits are shown in Figs. 1 and 2. Moreover, the following statements hold:*

(a) There are 12 *topologically distinct phase portraits in* $\mathbf{QsnSN_{11}(A)}$*. More precisely, we have* $H_2, H_3, H_4, H_5, H_6, H_{10}$ *plus the systems with the separatrix connection* $4V_1, 4V_2, 7V_1$*. Moreover, phase portraits* $5V_5, 5V_6$ *and* $5V_7$ *also belong to this family since the coalescence of two infinite singular points does not affect one of the double point at infinity. There is one generic region in the closure of* $\mathbf{QsnSN_{11}(A)}$*, namely* H_1*, whose phase portrait does not belong to* $\mathbf{QsnSN_{11}(A)}$*, since* H_1 *has two double complex singularities at infinity.*

(b) There are five phase portraits with more than one nondegenerate graphic, and they are in the parts $5V_5$*,* $5V_6$*,* $5V_7$*,* $2.5S_2$*,* $4.5S_3$*.*

(c) There are eight phase portraits with degenerate graphic, and they are in the parts $8V_1$*,* $2.8S_2$*,* $5.8S_1$*,* $5.8S_2$*,* $8.9S_1$*,* $2.8.9L_1$*,* $8.9.9L_1$*,* P_4*.*

(d) From the 36 *phase portraits, two of them (located in the border of* $\mathbf{QsnSN_{11}(A)}$*) correspond to linear systems. The corresponding phase portraits are given in Fig. 1.*

Corollary 1.2. *For the class* $\overline{\mathbf{QsnSN_{11}(A)}}$*, Table 1.1 compares the number of phase portraits possessing some geometrical features between the family* $\mathbf{QsnSN_{11}(A)}$ *and its border.*

Table 1.1. Comparison between the family $\mathbf{QsnSN_{11}(A)}$ and its border

	$\mathbf{QsnSN_{11}(A)}$	border of $\mathbf{QsnSN_{11}(A)}$
Distinct phase portraits	12	24
Phase portraits with more than one nondegenerate graphic	3	2
Phase portraits with degenerate graphics	0	8

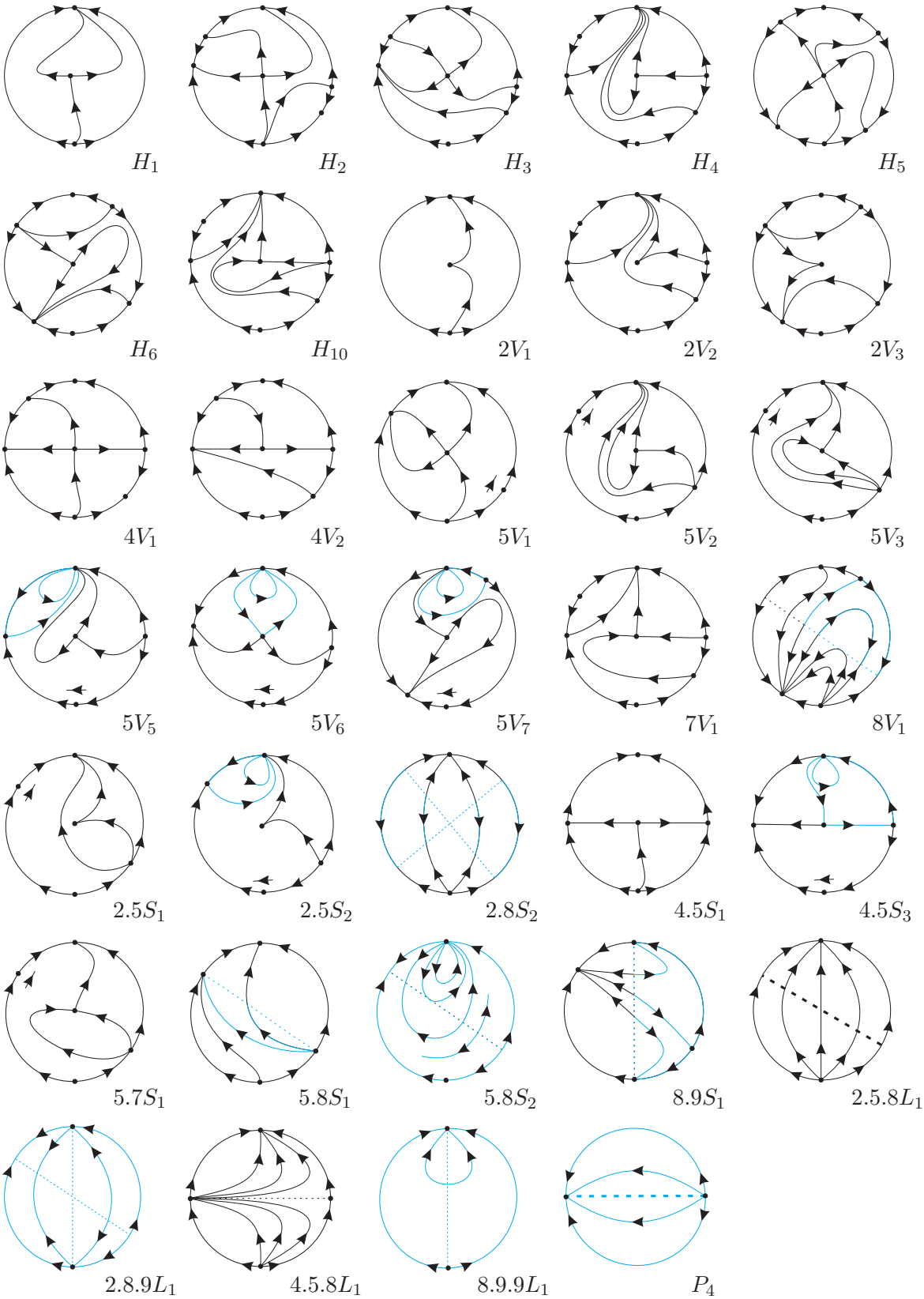

Fig. 2. Phase portraits for quadratic vector fields from class $\overline{\mathbf{QsnSN_{11}(A)}}$

From the 12 topologically distinct phase portraits of the family $\mathbf{QsnSN_{11}(A)}$, 6 occur in four–dimensional parts and 6 in three–dimensional parts.

From the remaining 24 phase portraits, which are on the border of $\mathbf{QsnSN_{11}(A)}$, one occurs in a four–dimensional part, seven occur in the three–dimensional parts, nine occur in the two–dimensional parts, five occur in the one–dimensional parts and two occur in the zero–dimensional parts.

In Figs. 1 and 2 we have illustrated all the singular points with a small disc. In case of degenerate systems we have also illustrated the infinite singular point belonging to the degenerate set with a small disc only if this point is an infinite singularity of the reduced system. We have drawn with thicker curves the separatrices and also the lines filled up with singularities which is double. We have added some thinner orbits to avoid confusion in some required cases. Moreover, we label the phase portraits according to the parts of the bifurcation diagram where they appear. Here we call *hypervolumes* (H) the four–dimensional parts of the bifurcation diagram, *volumes* (V) the three–dimensional ones, *surfaces* (S) the two–dimensional ones, *curves* (L) the one–dimensional ones, and *points* (P) the zero–dimensional ones.

As in [Artés *et al.*, 2006, Artés *et al.*, 2015], we use the same pattern in order to indicate the elements (V), (S), (L) and (P) in the bifurcation diagram. In this paper we indicate each one of the *hypervolumes* (H) surrounded by a circle, as in Fig. 6.

This paper is organized as follows. In Sec. 2 we present some incompatibilities found in previous classifications of phase portraits possessing specific properties on its singularities.

In Sec. 3 we describe some basic features regarding normal form (6) and we explain the structure of the bifurcation diagram.

In Sec. 4, using algebraic invariants and T–comitants as used by the Sibirskii School, we define the algebraic manifolds that describe the bifurcation diagram for the class $\overline{\mathbf{QsnSN_{11}(A)}}$.

In Secs. 5 and 6 we explain all the three–dimensional slices (and also the bifurcation planes on them) in the affine part and in the infinite of $\mathbb{RP}^4$, respectively.

In Sec. 7 we discuss about the possible existence of "islands" in the bifurcation diagram.

In Sec. 8 we introduce a global invariant denoted by $\mathcal{I}$, which classifies completely, up to topological equivalence, the phase portraits that we have obtained for the systems in the class $\overline{\mathbf{QsnSN_{11}(A)}}$. Theorem 8.7 shows clearly that they are uniquely determined (up to topological equivalence) by the values of the invariant $\mathcal{I}$.

The bifurcation diagram described in Secs. 5 and 6, plus Table 8.1 (from Sec. 8) of the geometrical invariants distinguishing the 34 phase portraits corresponding to quadratic systems, plus Table 8.2 giving the equivalences with the remaining phase portraits lead to the proof of the main statement of Theorem 1.1.

2. Some incompatibilities in previous classifications

It is quite common that by performing the study of a bifurcation diagram that produces some specific types of phase portraits, the authors lose one or several phase portraits. This may happen either because they do not interpret correctly some of the bifurcation parts or they miss the existence of some nonalgebraic bifurcations.

In this paper we have decided to start comparing our classification of phase portraits with existing classifications. We plan to do this section in every future work related to classification of phase portraits using normal forms. The aim of this study is to detect some incompatibilities in previous papers and also to help us look carefully our bifurcation diagram in order to not lose any phase portrait. Such incompatibilities are obtained after we compare all of the phase portraits obtained in our bifurcation diagram with phase portraits from some previous papers which possess the same *topological configuration of singularities*, according to Def. 1 from [Artés *et al.*, 2020b].

This study also allows the corresponding authors to detect possible mistakes on their works. There exist some previous papers which are not based on normal forms, but which seek all topological realizable phase portraits of a certain codimension (see [Artés *et al.*, 1998, Artés *et al.*, 2018, Artés *et al.*, 2019]). We have also crossed results from all the consulted papers with them and no discrepancy has been found.

In this present paper we are dealing with phase

portraits possessing only one finite double real singularity. Regarding the already existing classifications related to this paper, we know that in [Coll *et al.*, 1988a] one can find a classification of phase portraits of quadratic vector fields with only one finite singularity and in [Jager, 1990] the author presents a classification of phase portraits possessing a nilpotent cusp singularity of multiplicity two ($\widehat{cp}_{(2)}$). In some cases this is the only finite singularity, and thus, it may be present in our work (in the border of $\mathbf{QsnSN_{11}(A)}$). Then we have to verify if all of our nondegenerate phase portraits appear in one (or in both) papers. We also compare our phase portraits with those ones appearing in [Artés *et al.*, 2014, Artés *et al.*, 2015] when they must be present there. And also with [Artés *et al.*, 2006] as far as topological equivalence can be done.

By doing this comparison, we have detected some incompatibilities in some of the mentioned works. These incompatibilities are basically due to the presence of some phase portraits in our bifurcation diagram that does not appear in [Coll *et al.*, 1988a] or in [Jager, 1990]. We have also detected some minor misprints in [Artés *et al.*, 2006, Artés *et al.*, 2014, Artés *et al.*, 2015] but no missing phase portrait. Of course, we have not found any phase portraits in any of these papers which should be in our paper and was missing. Otherwise we would have already repaired that. This absence of phase portraits in [Coll *et al.*, 1988a, Jager, 1990] leads us to conclude that for some reason the authors have missed some cases and, consequently, the respective phase portraits.

In what follows we pass to describe a list of our phase portraits that allows us to identify such missing cases (or even some small mistakes) in the mentioned papers:

- Phase portraits H_{10} and $7V_1$ do not appear in [Coll *et al.*, 1988a]. In this case the authors missed the nonalgebraic bifurcation $7V_1$ and consequently the region beyond it.

- Phase portrait $2.5S_1$ does not appear in [Jager, 1990]. But we have detected that $2.5S_1$ corresponds to h_{18} from [Coll *et al.*, 1988a]. In this case Jager misses in Fig. 15 the possibility of λ_2 being zero, which leads to our phase portrait $2.5S_1$.

- We have also detected that phase portrait $5V_6$ corresponds to E_5 from [Coll *et al.*, 1988a], but E_5 has some drawing mistakes and it should be drawn exactly as our $5V_6$. In fact, there cannot exist an invariant straight line as drawn in [Coll *et al.*, 1988a] since the separatrix from the infinite saddle–node goes to the nodal part of the finite saddle–node in a different direction of the two separatrices of the finite singularity related to the nonzero eigenvalue.

The remaining phase portraits from Fig. 2 of this present paper corresponding to nondegenerate quadratic vector fields can be related to a phase portrait from [Coll *et al.*, 1988a] and those ones with a cusp in [Jager, 1990]. We highlight that both papers were done very close in time but none of the authors knew about the existence of the other work at that time and then they have not shared or even "crossed" their results. Another important fact that can support this claim is that phase portrait h_{15} from [Coll *et al.*, 1988a] does not appear in [Jager, 1990], and in fact it should appear in Fig. 6 of such a paper.

We have also analyzed the following four papers [Coll *et al.*, 1988a], [Artés *et al.*, 2006], [Artés *et al.*, 2014], and [Artés *et al.*, 2015]. As a result of this study we have detected that:

- Phase portrait V_1 from [Artés *et al.*, 2014] does not appear in [Coll *et al.*, 1988a]. In fact, phase portrait V_1 fits inside the class (I.s.12) of [Coll *et al.*, 1988a] but this class is not considered when they study cases with a semi–elemental finite singularity and two infinite singularities.

- Phase portrait $2.8L_1$ from [Artés *et al.*, 2015] corresponds to E_9 from [Coll *et al.*, 1988a], but E_9 also has some drawing mistakes and it should be drawn exactly as the mentioned $2.8L_1$. Indeed, the finite saddle is drawn as nilpotent when it must be elemental; as nilpotent [Coll *et al.*, 1988a] already has h_{14}.

- In Fig. 2 of [Artés *et al.*, 2006] there are two phase portraits called $2S_1$. According to the corresponding bifurcation diagram, we

observe that the second phase portrait which appears with this label should be called $2S_{11}$.

3. Quadratic vector fields with a finite saddle–node $\overline{sn}_{(2)}$ and an infinite saddle–node of type $\binom{\overline{1}}{1}SN$

As we mentioned before, for the class $\overline{\mathbf{QsnSN_{11}(B)}}$ (which will be presented in an independent paper), we will consider quadratic systems possessing a finite saddle–node $\overline{sn}_{(2)}$, a finite elemental singularity and an infinite saddle–node of type $\binom{\overline{1}}{1}SN$.

In this paper, for the class $\overline{\mathbf{QsnSN_{11}(A)}}$ we are considering that the mentioned finite elemental singularity has gone to infinity, i.e. we aim to study quadratic systems having only one finite saddle–node $\overline{sn}_{(2)}$ (which are located at the origin of the plane), an infinite saddle–node of type $\binom{\overline{1}}{1}SN$ and other infinite singularities, one of them of at least multiplicity two. Therefore, in this section we are considering quadratic systems of codimension at least three.

Using the T–comitants and invariants for quadratic systems as used by the Sibirskii school, in [Artés *et al.*, 2008] the authors have obtained two canonical forms for quadratic systems possessing one double real finite singularity and no more finite singularities; see Lemmas 3.24 and 3.25 from [Artés *et al.*, 2008]. In Table 6.1 from [Artés *et al.*, 2020a] these canonical forms are denoted by 16a and 16b, respectively. Family 16a is given by

$$\begin{aligned} \dot{x} &= dy + gx^2 + 2dxy, \\ \dot{y} &= fy + lx^2 + 2fxy, \end{aligned} \tag{5}$$

where d, f, g, l are real parameters and $fg - dl \neq 0$. On the other hand, family 16b is described by the differential equations

$$\begin{aligned} \dot{x} &= cx + dy, \\ \dot{y} &= lx^2 + 2mxy + ny^2, \end{aligned} \tag{6}$$

where c, d, l, m, n are real parameters and $ld^2 - 2cdm + nc^2 \neq 0$.

For both normal forms we have only one double finite singularity and the two other finite singularities have escaped to infinity. The geometric difference between them is that in normal form (5) both singularities coalesce with the same infinite singular point whereas in (6) they coalesce with different singular points. These facts are confirmed by Diagram 9.2 from [Artés *et al.*, 2020a], where we can observe that family 16a cannot produce an infinite singularity of type $\binom{\overline{1}}{1}SN$ whereas on family 16b one may obtain such a kind of infinite singularity in some of the branches of the diagram. Then, as our main goal is to make a global study of the class $\mathbf{QsnSN_{11}}$ of all real quadratic polynomial differential systems possessing a finite saddle–node $\overline{sn}_{(2)}$ and an infinite saddle–node of type $\binom{\overline{1}}{1}SN$, in this paper we provide the study of the canonical form (6).

We observe that canonical form (6) depends on five real parameters, namely, c, d, l, m and n. Then, its bifurcation diagram is actually the five–dimensional Euclidean space $\mathbb{R}^5$. Since the case $c = d = l = m = n = 0$ corresponds to the null systems and does not belong to our family, we can work with the real projective space $\mathbb{RP}^4$. We point out that this is the first time that a five–dimensional bifurcation diagram is studied using all the ideas and theory described, for instance, in [Artés *et al.*, 2006, Artés *et al.*, 2015]. In what follows we describe how we do this work.

Systems (6) depend on the parameter $\lambda = (c, l, m, d, n) \in \mathbb{R}^5$. We consider systems (6) which are nonzero, i.e. $\lambda = (c, l, m, d, n) \neq 0$. In this case, systems (6) can be rescaled with the affine transformation $(x, y, t) \to (x, y, \alpha t)$, $\alpha \neq 0$. In fact, applying this transformation we obtain

$$\begin{aligned} \dot{x} &= \alpha' cx + \alpha' dy, \\ \dot{y} &= \alpha' lx^2 + 2\alpha' mxy + \alpha' ny^2, \end{aligned}$$

for $\alpha' = 1/\alpha$, $\alpha \neq 0$. Then, this transformation takes the systems with parameters (c, l, m, d, n) to systems with parameters $(\alpha' c, \alpha' l, \alpha' m, \alpha' d, \alpha' n)$, with $\alpha' = 1/\alpha$. Hence, instead of taking $\mathbb{R}^5$ as parameter space, we may consider the real projective space $\mathbb{RP}^4$. The four–dimensional projective space $\mathbb{RP}^4$ can be viewed as the quotient space $\mathbb{S}^4/_\sim$ of $\mathbb{S}^4$ by the equivalence relation: (c, l, m, d, n) is equivalent to itself or to $(-c, -l, -m, -d, -n)$. So, our parameter is $[\lambda] = [c : l : m : d : n] \in \mathbb{RP}^4 = \mathbb{S}^4/_\sim$. Since for $\alpha' = -1$ the signs of all the parameters change, we may consider $d \geq 0$ in $[c : l : m : d : n]$. Since $c^2 + l^2 + m^2 + d^2 + n^2 = 1$,

then $d = \sqrt{1-(c^2+l^2+m^2+n^2)}$, where $0 \leq c^2+l^2+m^2+n^2 \leq 1$.

We can therefore view the parameter space as a ball: $\overline{\mathcal{B}} = \{(c,l,m,n) \in \mathbb{R}^4;\, c^2+l^2+m^2+n^2 \leq 1\}$ where on the border of this ball, two opposite points are identified. So, we are working with a four–dimensional space. The studies done up to now like [Artés *et al.*, 2006, Artés *et al.*, 2015] were done in a three–dimensional space. The parameter space was divided in specific two–dimensional slices which were of interest for the bifurcation. In our case we must divide the parameter space into three–dimensional slices which later must also be divided into two–dimensional planes in order to be drawn on a paper. We will see that the number of three–dimensional slices (and also the number of planes) is very small. Anyway, as we have mentioned before, this is the first time that this study is done and it is of great interest to have clear ideas when working at this level of dimensions. The different three–dimensional slices that we will detect share one common "top" which can be considered as an $\mathbb{RP}^2$. We have already chosen the parameter d as the parameter to distinguish from the affine space and the infinity. We will chose parameter n to foliate $\mathbb{RP}^4$ into three–dimensional spaces. And we will chose parameter m to split each three–dimensional space into two–dimensional spaces. The complete and general set can be seen as in Fig. 3, where the different k, k_0, k_1, k_α can be a single number or several different numbers if more slices are needed. If more slices were needed, the different cases would correspond alternatively to generic and singular slices. Since systems (6) show different types of symmetries, whenever we change the sign of any of the parameters, each parameter equal to zero will correspond to a singular slice. We will use the parameters c and l as Cartesian coordinates to draw the bifurcation diagram in two dimensions. So, the most simple bifurcation diagram will have at least eight slices of different dimensions. In fact, this will be our case. These slices correspond to the different cases $(d,m,n) \in \{(0,0,0),(0,0,1),(0,1,0),(1,0,0),(0,1,1),(1,0,1),(1,1,0),(1,1,1)\}$. In Fig. 3 we present a general scenario of the partition of the bifurcation diagram.

For $d \neq 0$, we get the affine chart:

$$\mathbb{RP}^4 \setminus \{d=0\} \leftrightarrow \mathbb{R}^4$$
$$[c:l:m:d:n] \to \left(\frac{c}{d}, \frac{l}{d}, \frac{m}{d}, \frac{n}{d}\right) = (\overline{c}, \overline{l}, \overline{m}, \overline{n})$$
$$[\overline{c}:\overline{l}:\overline{m}:1:\overline{n}] \leftarrow (\overline{c}, \overline{l}, \overline{m}, \overline{n})$$

The subspace $d=0$ in $\mathbb{RP}^4$, which is an $\mathbb{RP}^3$, corresponds to the equation $c^2+l^2+m^2+n^2=1$ (that is, the full sphere $\mathbb{S}^3$ with identification of symmetrical points on the border).

When two parameters are zero, for example, $d=n=0$, we identify the point $[c:l:m:0:0] \in \mathbb{RP}^4$ with $[c:l:m] \in \mathbb{RP}^2$. So, this subset $\{d=n=0\} \subset \overline{\mathcal{B}}$ can be identified with $\mathbb{RP}^2$, which can be viewed as a disc with two opposite points on the circumference (the equator) identified.

Now, when three parameters are zero, for example, the plane $m=d=n=0$ in $\mathbb{RP}^4$ corresponds to the equation $c^2+l^2=1$ which is an $\mathbb{RP}^1$ space, that is a circle with the opposite points identified. The concept of equator which was used in bifurcations in $\mathbb{RP}^3$ (as for instance in [Artés *et al.*, 2006, Artés *et al.*, 2015]) now needs to be enlarged to "equators" of dimension two. More precisely, a one–dimensional equator is when all parameters, except two, are zero. A two–dimensional equator is when all, except three parameters, are zero.

Proposition 3.1. *By a rescaling in the variables, we may assume $d=0$ or $d=1$ in the normal form* (6).

Proof. If $d \neq 0$, by the reparametrization theorem we get that systems (6) are equivalent to

$$\begin{aligned} \dot{x} &= Cx + y, \\ \dot{y} &= Lx^2 + 2Mxy + Ny^2, \end{aligned}$$

where $C = c/d, L = l/d$, $M = m/d$ and $N = n/d$. By renaming the coefficients $C \to c$, $L \to l$, $M \to m$ and $N \to n$, we obtain systems (6) with $d=1$. Moreover, we must also consider the case when $d=0$. ∎

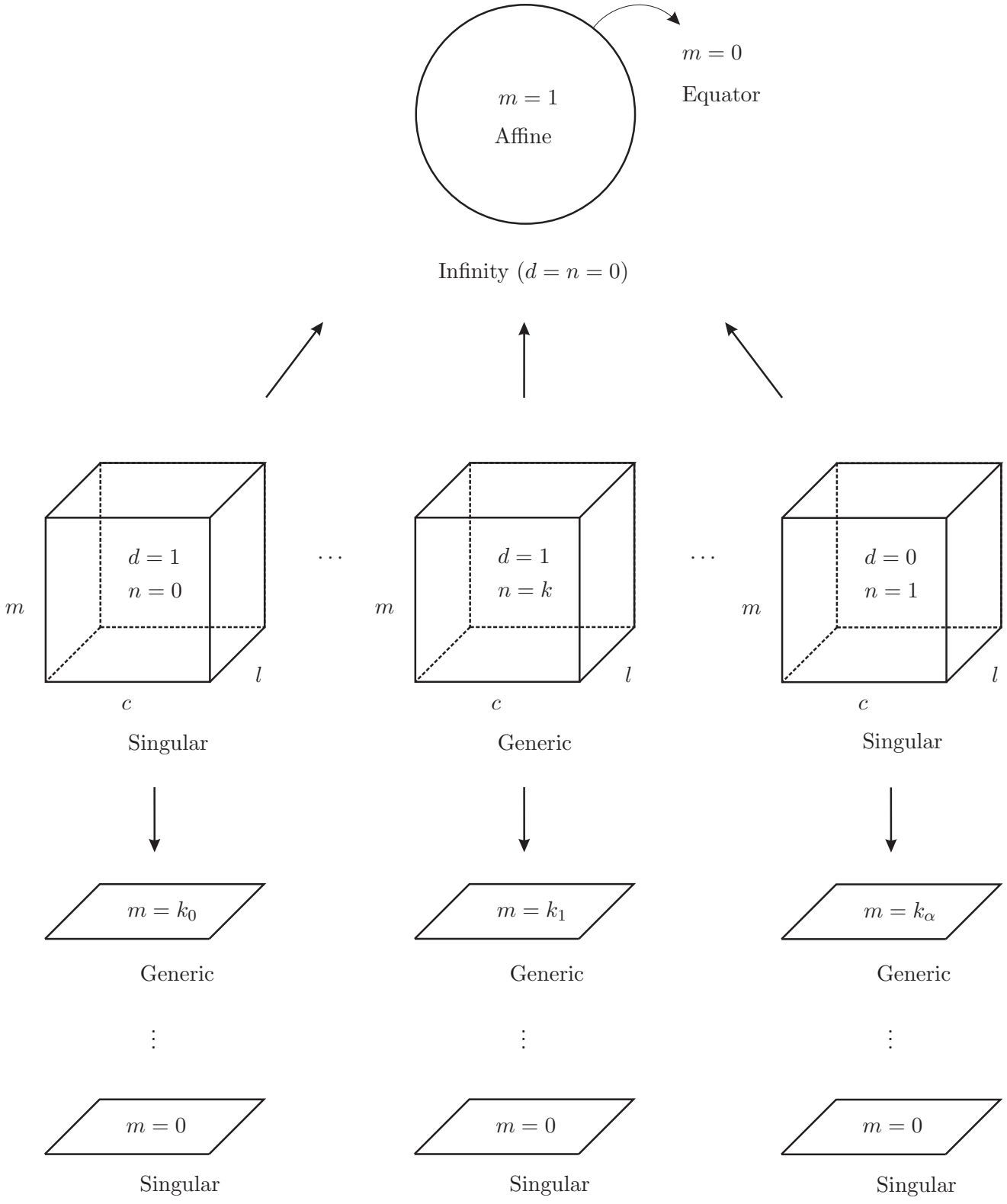

Fig. 3. Scheme of the partition of the bifurcation diagram. The parameter $d = 1$ (respectively $d = 0$) represents the affine (respectively infinite) part of $\mathbb{RP}^4$, the three–dimensional slices are given by the parameter n and from each three–dimensional slice the parameter m indicates the planes that must be studied

4. The bifurcation diagram of the systems in $\overline{\mathbf{QsnSN_{11}(A)}}$

In order to construct the bifurcation diagram for systems (6), in this paper we consider the concepts of algebraic invariants and T–comitants as formulated by the Sibirskii school for differential equations. For a quick summary see for instance Sec. 7 of [Artés *et al.*, 2006].

4.1. Algebraic manifolds in $\mathbb{RP}^4$

According to Diagram 9.2 from [Artés *et al.*, 2020a], here we define the algebraic manifolds that are needed for the study of the bifurcation diagram of canonical form (6). These manifolds are given by the invariants and comitants listed in such a diagram.

Bifurcation manifold in $\mathbb{RP}^4$ due to degeneracy of systems

$(\mathcal{V}_8)$ Since for systems (6) we have a double real finite singularity and two finite singularities have coalesced with different singularities at infinity, according to Diagram 9.2 from [Artés *et al.*, 2020a] one must have $\mu_0 = \mu_1 = \kappa = 0$ and $\mu_2 \neq 0$. Additionally, calculations show that $\mu_3 = \mu_4 = 0$ and

$$\mu_2 = (ld^2 - 2cdm + nc^2)(lx^2 + 2mxy + ny^2).$$

So we define $(\mathcal{V}_8)$ as a manifold whose equation is equivalent to $\mu_2 = 0$, i.e.

$$(\mathcal{V}_8)\colon ld^2 - 2cdm + nc^2 = 0,$$

and therefore on this manifold we have $\mu_i = 0$, $i = 0, 1, 2, 3, 4$, i.e. systems (6) are degenerate.
We point out that our aim is to construct a coherent and continuous bifurcation diagram. Although the phase portraits possessing a double finite saddle–node $\overline{sn}_{(2)}$ and an infinite saddle–node $\left(\overline{1}\right)SN$, belong to open sets in this bifurcation diagram, in order to have these properties for this diagram, we also need to consider the borders of such sets. In particular, manifold $(\mathcal{V}_8)$ borders open sets in this bifurcation diagram.

Remark 4.1. According to Diagram 9.2 from [Artés *et al.*, 2020a] the comitant

$$\widetilde{L} = 8n(lx^2 + 2mxy + ny^2),$$

multiplied by μ_2, allows us to distinguish between different configurations of infinite singularities. More precisely, we have

$$\mu_2\widetilde{L} = 8n(ld^2 - 2cdm + nc^2)(lx^2 + 2mxy + ny^2)^2,$$

and if $\mu_2\widetilde{L} < 0$ we have the configuration of singularities $\left(\overline{1}\right)SN$, $\left(\overline{1}\right)SN$, N and if $\mu_2\widetilde{L} > 0$ we have the configuration of singularities $\left(\overline{1}\right)SN$, $\left(\overline{1}\right)NS$, N.

Remark 4.2. In some of the following manifolds the factor $ld^2 - 2cdm + nc^2$ is also present. This confirms that the systems on manifold $(\mathcal{V}_8)$ are indeed degenerate (possessing curves of singularities) because many geometrical features happen at the same time when $ld^2 - 2cdm + nc^2 = 0$. However, we are interested in the other geometrical features that the following manifolds can provide. In this way, we assume, without loss of generality, that $ld^2 - 2cdm + nc^2 \neq 0$.

Bifurcation manifold in $\mathbb{RP}^4$ due to the change of topological type of the origin

$(\mathcal{V}_2)$ This is the bifurcation manifold due to the change of topological type of the origin. On this manifold the origin becomes a cusp–type singularity. This phenomenon occurs when two separatrices of a saddle–node coalesce. A necessary condition for this phenomenon to happen is that the trace of the Jacobian of the finite singularity is zero and it is described by the invariant

$$\mathcal{T}_4 = 4c^2n(d^2l - 2cdm + c^2n)(-m^2 + ln).$$

Taking into consideration Remark 4.2, we define manifold $(\mathcal{V}_2)$ by

$$(\mathcal{V}_2)\colon c^2n(-m^2 + ln) = 0.$$

Remark 4.3. We observe that for $n = 0$, we have $(\mathcal{V}_2) \equiv 0$. According to Diagram 9.2 from [Artés *et al.*, 2020a] we must consider the comitant

$$\widetilde{M}\Big|_{n=0} = -32m^2x^2,$$

which vanishes if and only if $m = 0$. Such a mentioned diagram tells us that when $n = 0$ and $m \neq 0$ we can consider the invariant

$$\mathcal{B}_1\Big|_{n=0} = -2c^2dm(-dl + 2cm),$$

and when $n = m = 0$ we can consider the comitant

$$\mathcal{B}_4\Big|_{n=m=0} = 6clx^2(cx + dy).$$

Due to Remark 4.2 and the diagram under discussion, for $n = 0$ we can define

$$(\mathcal{V}_2)\colon c^2m = 0 \quad \text{if} \quad m \neq 0, \tag{7}$$

and

$$(\mathcal{V}_2)\colon c = 0 \quad \text{if} \quad m = 0. \tag{8}$$

Bifurcation manifold in $\mathbb{RP}^4$ due to the presence of invariant straight lines

$(\mathcal{V}_4)$ This manifold in $\mathbb{RP}^4$ will contain the points of the parameter space where invariant straight lines appear. These straight lines may contain connections of separatrices from different singularities or not. So, in some cases, it may imply a topological bifurcation or not. According to Corollary 4.6 from [Schlomiuk & Vulpe, 2004] we have necessary conditions for the existence of invariant straight lines, which are given in terms of the zeroes of the comitants B_1, B_2, and B_3. More precisely, such a result tells us that for the existence of an invariant straight line in one (respectively two or three distinct) directions in the affine plane it is necessary that $B_1 = 0$ (respectively $B_2 = 0$ or $B_3 = 0$). Calculations yield

$$\begin{aligned} B_1 &= 0, \\ B_2 &= -648l^2(ld^2 - 2cdm + nc^2)^2x^4, \\ B_3 &= -6(d^2l - 2cdm + c^2n)x^2y(lx + my). \end{aligned}$$

Taking into consideration Remark 4.2, we conclude that B_1 is identically zero, B_2 is equivalent to $l = 0$ and B_3 is nonzero. In the case when B_1 is not identically zero, we can simply rely on the bifurcation $B_1 = 0$ to look for the possible existence of invariant straight lines (as for instance in [Artés *et al.*, 2015]). However, in this case when $B_1 \equiv 0$, we have an invariant line which coalesced with the infinite line $Z = 0$ (i.e. this line is a double one), and we may have invariant straight lines in other directions. Any single affine straight line can be considered "parallel" to the infinity line. Then the invariant $B_2 \equiv 0$ may not cover all the possibilities of existence of a second line. So, we must do the detailed study of whether there can exist or not straight lines. Doing this study it is easy to determine that any invariant straight line must cross the origin and they will exist if $l = 0$ or if $ld^2 - 2cdm + nc^2 = 0$ (see Lemma 4.4). These are exactly the components of B_2 plus the component $d = 0$. We define manifold $(\mathcal{V}_4)$ by the equation

$$(\mathcal{V}_4)\colon dl(ld^2 - 2cdm + nc^2) = 0.$$

Lemma 4.4. *Systems* (6) *possess the following invariant straight lines under specific conditions:*

(i) $\{y = 0\}$, *if* $l = 0$;

(ii) $\{x = 0\}$, *if* $d = 0$;

(iii) $\{ax + by = 0\}$, *if* $d = cb/a$ *and* $n = (2mab - lb^2)/a^2$, *for* $a \neq 0$. *Moreover, these values of* d *and* n *satisfy the equation* $ld^2 - 2cdm + nc^2 = 0$, *i.e. we have degenerate systems.*

Proof. We consider the algebraic curves

$$\begin{aligned} f_1(x, y) &\equiv y = 0, \\ f_2(x, y) &\equiv x = 0, \\ f_3(x, y) &\equiv ax + by = 0, \end{aligned}$$

and we show that the polynomials

$$\begin{aligned} K_1(x, y) &= 2mx + ny, \\ K_2(x, y) &= c, \\ K_3(x, y) &= c + \frac{lb}{a}x + \frac{b(2ma - lb)}{a^2}y, \end{aligned}$$

are the cofactors of $f_1 = 0$, $f_2 = 0$, and $f_3 = 0$, respectively, after restricting systems (6) to the respective conditions. ■

In this work we shall detect another bifurcation manifold that is not necessarily algebraic and on which the systems have connection of separatrices different from that ones given by $(\mathcal{V}_4)$. The equations of this bifurcation manifold can only be determined approximately by means of numerical tools and its existence is proved by using arguments of continuity in the bifurcation diagram. We shall name this manifold $(\mathcal{V}_7)$.

Bifurcation manifold in $\mathbb{RP}^4$ due to multiplicities of infinite singularities

$(\mathcal{V}_5)$ This is the bifurcation manifold due to the coalescence of infinite singularities. This phenomenon is detected by the invariant η which is given by

$$\eta = -4n^2(-m^2 + ln) = 0.$$

We define manifold $(\mathcal{V}_5)$ by the equation

$$(\mathcal{V}_5)\colon n^2(-m^2+ln)=0.$$

Remark 4.5. Again we observe that for $n=0$, we have $(\mathcal{V}_5)\equiv 0$. According to Diagram 9.2 from [Artés *et al.*, 2020a] we must consider the comitant

$$\widetilde{M}\Big|_{n=0}=-32m^2x^2,$$

which vanishes if and only if $m=0$. Such a mentioned diagram tells us that when $n=0$ we can define

$$(\mathcal{V}_5)\colon m=0 \quad \text{if} \quad n=0. \tag{9}$$

We will see that on the slice $n=0$ we will always have a coalescence of infinite singularities.

As we said before, we work at the chart of $\mathbb{RP}^4$ corresponding to $d\neq 0$, and we take $d=1$. In order to perform the analysis, we shall use pictures which are drawn on planes of $\mathbb{RP}^4$, having coordinates $[c:l:m_0:1:n_0]$, with n_0 and m_0 constants, plus the open half sphere $d=0$ and we shall give pictures of the resulting bifurcation diagram on these planar sections on a disc or in an affine chart of $\mathbb{R}^2$. In these planes the coordinates are (c,l) where the horizontal line is the c–axis.

As in [Artés *et al.*, 2006, Artés *et al.*, 2015], in this paper we use colors to refer to the bifurcation manifolds:

(a) manifold $(\mathcal{V}_2)$ is drawn in green (the origin becomes a cusp–type singularity);

(b) the nondegenerate part of manifold $(\mathcal{V}_4)$ is drawn in purple (presence of at least one invariant straight line). We draw it as a continuous curve if it implies a topological change or as a dashed curve otherwise;

(c) manifold $(\mathcal{V}_5)$ is drawn in red (two infinite singular points coalesce);

(d) manifold $(\mathcal{V}_7)$ is also drawn in purple (connections of separatrices); and

(e) manifold $(\mathcal{V}_8)$ is drawn in cyan (the systems are degenerate).

We use the same color for $(\mathcal{V}_4)$ and $(\mathcal{V}_7)$ since both manifolds deal with connections of separatrices.

4.2. Geometric features of the algebraic manifolds in $\mathbb{RP}^4$

Before we pass to the study of the geometric features of manifolds $(\mathcal{V}_2)$, $(\mathcal{V}_4)$, $(\mathcal{V}_5)$, and $(\mathcal{V}_8)$, first we remember the definition of a singularity of a several variables smooth map.

Definition 4.6. Let $f: U\subset\mathbb{R}^m\to\mathbb{R}^n$ be a smooth map. A point $p\in U$ is a **singular point** of f if the rank of the Jacobian matrix $Df(p)$ is strictly less than $\min(m,n)$. More precisely, given $f=(f_1,\dots,f_n): U\subset\mathbb{R}^m\to\mathbb{R}^n$ with $f_i=f_i(x_1,\dots,x_m), i=1,\dots,n$, we say that $p\in U$ is a **singular point** for f if the matrix

$$\begin{bmatrix} \frac{\partial f_1}{\partial x_1} & \cdots & \frac{\partial f_1}{\partial x_m} \\ \vdots & \ddots & \vdots \\ \frac{\partial f_n}{\partial x_1} & \cdots & \frac{\partial f_n}{\partial x_m} \end{bmatrix}(p)$$

has rank $r<\min(m,n)$.

We have defined the following manifolds

$$\begin{aligned}
&(\mathcal{V}_8)\colon n(ld^2-2cdm+nc^2)=0,\\
&(\mathcal{V}_2)\colon c^2n(-m^2+ln)=0,\\
&(\mathcal{V}_4)\colon l=0,\\
&(\mathcal{V}_5)\colon n^2(-m^2+ln)=0.
\end{aligned}$$

Here we are interested in studying the geometrical behavior of all of these manifolds, that is, their singularities (according to Def. 4.6), their intersection points and their "tangencies" (in the affine space) with three–dimensional slices of the type $d=1$ and constant n. Since this study requires a lot of computations which would take a very large number of pages to present all the details, in order to be more succinct we have developed an algorithm in software Mathematica and we have created a notebook with all the computations on it. This algorithm will be available for free download through the link `http://mat.uab.cat/~artes/articles/qvfsn2SN11A/sn2SN11A.nb` (some previous knowledge of Mathematica is recommended for using this algorithm).

In what follows, we describe the main idea of what we have done in this subsection and we present the results. For more details we recommend the mentioned Mathematica algorithm.

Remark 4.7. In $\mathbb{R}^5$ we will create a list of k–dimensional objects, $1 \leq k \leq 4$, in the following way. We denote by $\{Okx_{i(k)}\}_{\{1\leq k\leq 4,\ i(k)\in\mathbb{N}\}}$ a list of k–dimensional objects, where each $Okx_{i(k)}$ is a list of objects of dimension $k \in \{1,\ldots,4\}$. For instance, $O4x_1$ stands for the first element of the list of four–dimensional objects. By "dimension" of an object we mean the number of parameters used for defining it.

In order to proceed with the study of all geometric features (of the manifolds) described before, it is interesting to work with the components of each manifold (this idea was used explicitly in [Artés *et al.*, 2006, Artés *et al.*, 2015]). Then we generate a list of four–dimensional components, which are denoted according to Remark 4.7:

- $O4x_1 : c = 0$ which corresponds to the set $\{0, l, m, d, n\}$;
- $O4x_2 : l = 0$ which corresponds to the set $\{c, 0, m, d, n\}$;
- $O4x_3 : n = 0$ which corresponds to the set $\{c, l, m, d, 0\}$;
- $O4x_4 : m^2 - ln = 0$ which corresponds to the set $\{c, l, m, d, m^2/l\}$;
- $O4x_5 : ld^2 - 2cdm + c^2n = 0$ which corresponds to the set $\{c, (2cdm - nc^2)/d^2, m, d, n\}$;

Now we proceed with the study of the singularities of the four–dimensional components (i.e. the objects $O4x_i, i = 1,\ldots,5$) and their respective intersections. We will also study the "tangencies" of these objects in the affine space with slices of the type $d = 1$ and constant n. This study generates a set of three–dimensional or lower objects. Concretely, we have the new objects:

- $O3x_1 = \{0, 0, m, d, n\}$;
- $O3x_2 = \{0, l, m, 0, n\}$;
- $O3x_3 = \{0, l, m, d, 0\}$;
- $O3x_4 = \{0, l, m, d, m^2/l\}$;
- $O3x_5 = \{0, l, m, d, dm^2/l\}$;
- $O3x_6 = \{c, 0, 0, d, n\}$;
- $O3x_7 = \{c, 0, m, d, 0\}$;
- $O3x_8 = \{c, 0, m, d, 2dm/c\}$;
- $O3x_9 = \{c, 0, cdn/2, d, n\}$;
- $O3x_{10} = \{c, l, 0, d, 0\}$;
- $O3x_{11} = \{c, l, dl/2c, d, 0\}$;
- $O3x_{12} = \{c, l, m, 0, 0\}$;
- $O3x_{13} = \{c, cm/d, m, d, dm/c\}$;
- $O3x_{14} = \{c, c^2dn, cdn, d, n\}$;
- $O2x_1 = \{0, 0, 0, d, n\}$;
- $O2x_2 = \{0, 0, m, d, 0\}$;
- $O2x_3 = \{0, l, m, 0, m^2/l\}$;
- $O2x_4 = \{c, 0, 0, d, 0\}$;
- $O2x_5 = \{c, l, 0, 0, 0\}$;
- $O1x_1 = \{0, 0, 0, 0, n\}$.

Now we take the list of three–dimensional objects $O3x_i$ and we study their singularities and their respective intersections. We will also study the possibility that any of these objects may be expressed by means of square roots which could produce the change from real solutions to complex ones under some conditions. This generates a set of two–dimensional or lower objects which enlarge the set previously found. Concretely, we have added the new objects:

- $O2x_6 = \{0, 0, m, 0, n\}$;
- $O2x_7 = \{0, l, 0, d, 0\}$;
- $O2x_8 = \{0, l, m, 0, 0\}$;
- $O2x_9 = \{c, 0, 0, 0, n\}$;
- $O2x_{10} = \{c, 0, m, 0, 0\}$;
- $O1x_2 = \{0, 0, 0, d, 0\}$;
- $O1x_3 = \{0, 0, m, 0, 0\}$;
- $O1x_4 = \{0, l, 0, 0, 0\}$;
- $O1x_5 = \{c, 0, 0, 0, 0\}$.

Now we take the list of two–dimensional objects $O2x_i$ and we study their singularities and their respective intersections. Again we consider the possibility of the presence of square roots, which imply real or complex solutions under some conditions. This generates a set of one–dimensional objects which enlarge the set previously found. But we do not have any new element, since we detect that the elements obtained at this stage have already been found previously.

Now, these five one–dimensional objects, which are in $\mathbb{R}^5$ correspond to points in the projective space, which will determine the singular slices that we must take into consideration. As we have said, the bifurcation diagram is very simple and it is described by the next lemma.

Lemma 4.8. *The parameter space of systems* (6)*, which is an* $\mathbb{RP}^4$*, bifurcates into three spaces* $\mathbb{RP}^3$ *which are* $[c : l : m : 1 : 1]$ *(generic),* $[c : l : m : 1 : 0]$ *and* $[c : l : m : 0 : 1]$ *(both singular). Then, inside each one of these three–dimensional slices we must only consider two cases:* $m = 1$ *(generic) and* $m = 0$ *(singular). Finally, the space* $\mathbb{RP}^2$ *is given by* $[c : l : m : 0 : 0]$ *which is border of* $[c : l : m : 0 : 1]$.

Even although we have found the existence of a nonalgebraic bifurcation, we have not detected that more slices are needed because of it, i.e. there is complete coherence of continuity of the phase portraits with the slices already provided.

We now begin the analysis of the two–dimensional bifurcation diagrams by studying completely each one of the elements described in Lemma 4.8.

We describe first the labels used for each part of the bifurcation space. As we have mentioned before, the subsets of dimensions 4, 3, 2, 1 and 0, of the partition of the parameter space will be denoted respectively by H, V, S, L and P for Hypervolume, Volume, Surface, Line and Point, respectively. The volumes are named using a number which corresponds to each bifurcation volume which is placed on the left side of the letter V and in order to describe the portion of the volume we place an index. The surfaces that are intersection of volumes are named by using their corresponding numbers on the left side of the letter S, separated by a point. The surfaces which are singularities of volumes are named by using the number of the surface twice on the left side of the letter S. To describe the piece of the surface we place an index. The curves that appear can come from different sources: they could be intersection of surfaces, intersection among several volumes, singularities of volumes, and, in general, any object of this classification of dimension one. The curves are named by using their corresponding numbers (of the volumes containing them) on the left side of the letter L, separated by a point. In case we have more than three volumes intersecting on the same curve, we place the three numbers of the surfaces that we consider more relevant. To describe the segment of the curve we place an index. Hypervolumes and Points are simply indexed.

We consider an example: variety $(\mathcal{V}_2)$ splits into 3 different three–dimensional parts labeled as $2V_1$, $2V_2$ and $2V_3$, plus some two–dimensional parts labeled as $2.iS_j$ (where i denotes the other volume intersected by $(\mathcal{V}_2)$ and j is a number), plus some one–dimensional parts labeled as $2.i.kL_j$ (where i and k denote the other volumes intersected by $(\mathcal{V}_2)$ and j is a number), and also some zero–dimensional parts. In order to simplify the labels in all figures we see **H1** which stands for the TEX notation H_1. Analogously, **2V1** (respectively, **2.5S1**) stands for $2V_1$ (respectively, $2.5S_1$). And the same happens with many other pictures.

5. Bifurcation diagram in the affine part of $\mathbb{RP}^4$

Here we assume that $d = 1$ and we have to consider the three–dimensional slices $n = 1$ and $n = 0$, which indicate, respectively, a generic and a singular slice for $d = 1$.

In Fig. 4 we represent the generic plane $m = 1$ of the parameter space for the generic slice $n = 1$, showing only the algebraic surfaces. We will use lower–case letters provisionally to describe the sets found algebraically in order to not interfere with the final partition described with capital letters. Moreover, we obtain the global phase portraits with the numerical program P4 [Artés *et al.*, 2005, Dumortier *et al.*, 2006]. In this slice we have a partition in two–dimensional parts bordered by curved polygons, some of them bounded, others bordered by infinity. For each two–dimensional part we obtain a phase portrait which is coherent with those

of all their borders. Except for the part h_9 (the rectangle bordered by green, purple, red and infinity). The study of this part is very important for the coherence of the bifurcation diagram. That is why we have decided to present only this part (and its borders) in Fig. 4.

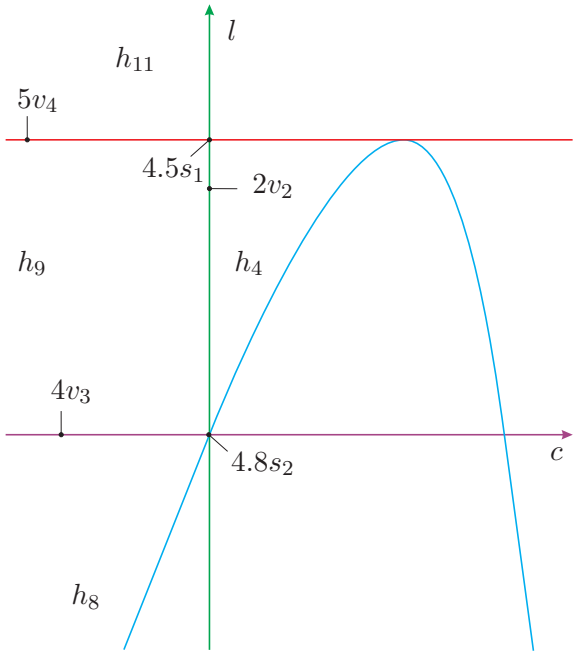

Fig. 4. Plane $m = 1$ on the slice $n = 1$ (only algebraic manifolds)

We start the analysis of part h_9. The phase portrait in h_9 near $2v_2$ possesses a finite basin passing through the finite saddle–node, i.e. two separatrices of the finite saddle–node start at the same infinite saddle–node, whereas the phase portrait in h_9 away from $2v_2$ does not possess the finite basin. Then, there must exist at least one element $7V_1$ of manifold $(\mathcal{V}_7)$ dividing part h_9 into two "new" parts, H_9 and H_{10}, which represents a bifurcation due to the connection of a separatrix of a finite saddle–node and a separatrix of an infinite saddle–node (see Fig. 5 for a sequence of phase portraits in these parts). As the segment $5v_4$ corresponds to changes in the infinite singular points, the finite part of the phase portraits remains unchanged and this element of nonalgebraic manifold $(\mathcal{V}_7)$ must intersect $5v_4$ having this intersection point as one of its endpoints, since in h_{11} we do not have the sufficient number of infinite singularities in order to make this nonalgebraic bifurcation to happen. In Lemma 5.1 we prove that $7V_1$ is bounded and it has $4.8s_2$ and $5.7S_1$ as endpoints. The complete bifurcation diagram for the generic plane $m = 1$ on the slice $n = 1$ is presented in Fig. 6.

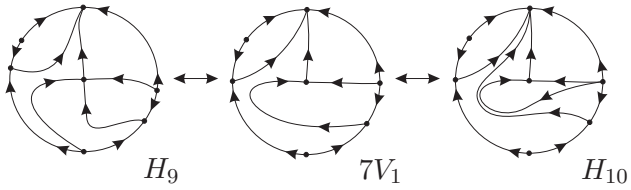

Fig. 5. Sequence of phase portraits in part h_9 of $n = m = 1$

Lemma 5.1. *The element $7V_1$ of variety $(\mathcal{V}_7)$ is bounded and it has $4.8s_2$ and $5.7s_1$ as endpoints.*

Proof. Numerical tools show that this result is true. We have mentioned earlier that in H_{11} we do not have the sufficient number of infinite singularities in order to make the nonalgebraic bifurcation given by $7V_1$ to happen. However, $7V_1$ must intersect $5v_4$ in some point, since some two different phase portraits $5V_3$ and $5V_4$ are detected on this part. Then such a manifold has an endpoint at $5.7S_1$. On the other hand, we observe that $4V_3$ represents the existence of an invariant straight line which indicates a topological change between H_8 and H_9. If some point of $4V_3$ were an endpoint of $7V_1$, then the invariant line would necessarily be broken in order to make this nonalgebraic bifurcation to happen. Then the second endpoint of $7V_1$ cannot be on $4V_3$. Moreover, it also cannot be on $2V_2$ since on such a manifold the finite saddle–node has become a cusp–type singularity. Therefore, the second endpoint of $7V_1$ is $4.8S_2$. See Fig. 6 for the mentioned regions in this proof. ■

For the slice $n = 1$, the only singular plane is $m = 0$, in which we observe that the volume regions $4V$ and $5V$ coalesce, making the hypervolume regions H_2, H_3, H_4, H_9, and H_{10} to disappear, see Fig. 7.

We now pass to the singular slice $n = 0$. According to the study of the geometrical features of the manifolds, we must consider the planes $m = 1$ and $m = 0$, which are, respectively, generic and singular planes for this slice.

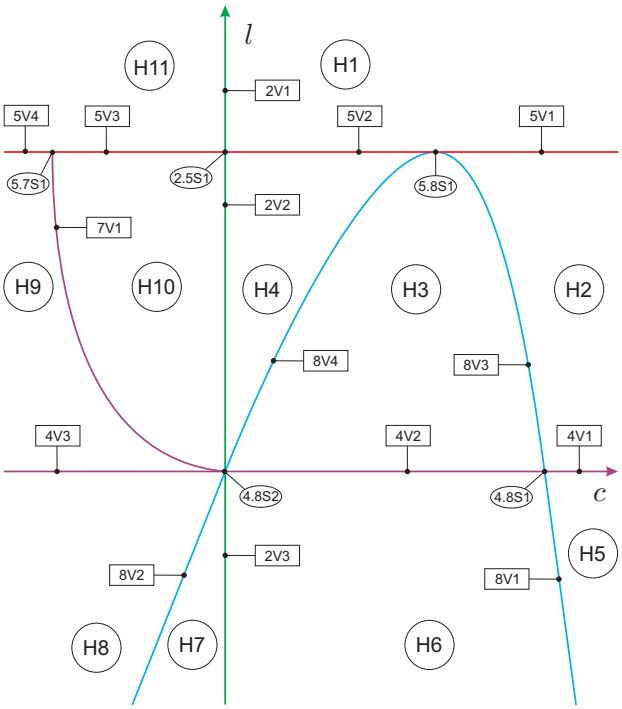

Fig. 6. Plane $m = 1$ on the slice $n = 1$

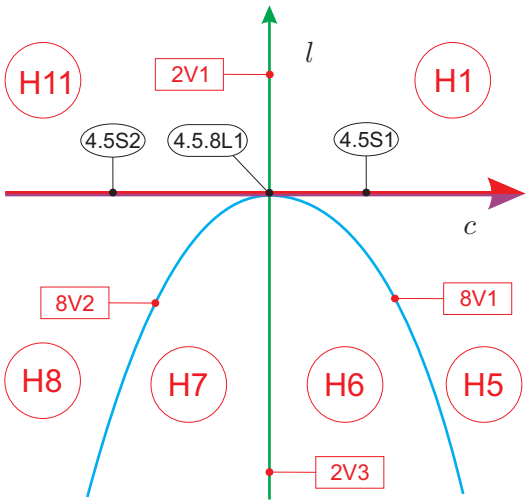

Fig. 7. Plane $m = 0$ on the slice $n = 1$ (see Fig. 6)

We start studying the generic plane $m = 1$. According to Remark 4.5, for this generic plane we have that $(\mathcal{V}_5) \equiv 0$, i.e, there are two infinite singularities that always coalesce. Moreover, in this case we have that $(\mathcal{V}_8)$ is reduced to the line $l = 2c$. In fact, almost all phase portraits from this value of the parameters d, n, m can be obtained from the previous ones via a specific coalescence of infinite singularities. We only have five exceptions, which are the parts which were gone to the infinity during the transition between the generic slice $m = 1$ and the singular one: H_1, H_2, H_5, H_9, and H_{11}. In Fig. 8 we have drawn this generic plane.

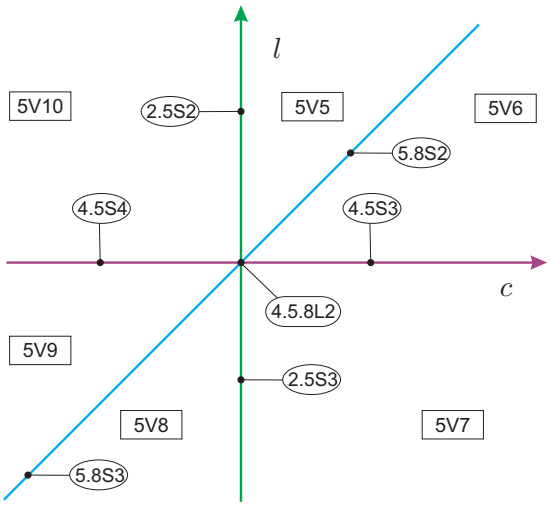

Fig. 8. Plane $m = 1$ on the slice $n = 0$ (see Fig. 7)

Now we discuss the singular plane $m = 0$. In this case, variety $(\mathcal{V}_8)$ is reduced to the line $l = 0$ and this movement makes the volume regions $5V_6$ and $5V_9$ disappear. The new corresponding regions are $4.5.8L_1$, $4.5.8L2$ and P_1 (see the representation of the plane $m = 0$ in Fig. 9). Moreover, since we are considering $n = 0$, according to Remark 4.5, for this singular plane we already have that $(\mathcal{V}_5) \equiv 0$. In addition, equation (9) tells us that $\widetilde{M}$ is also 0. Therefore, the phase portraits for the remaining regions of the plane $m = 0$ can be obtained from the corresponding phase portraits from the plane $m = 1$ by performing a convenient coalescence of infinite singularities. In Fig. 9 we have drawn this singular plane.

6. Bifurcation diagram in the infinite part of $\mathbb{RP}^4$

Here we assume that $d = 0$ and again we have to consider the three–dimensional slices $n = 1$ and $n = 0$, which now indicate, respectively, the affine and the infinite part of the infinity of $\mathbb{RP}^4$.

First we consider slice $n = 1$. In this slice we must perform the study of the planes $m = 1$ and

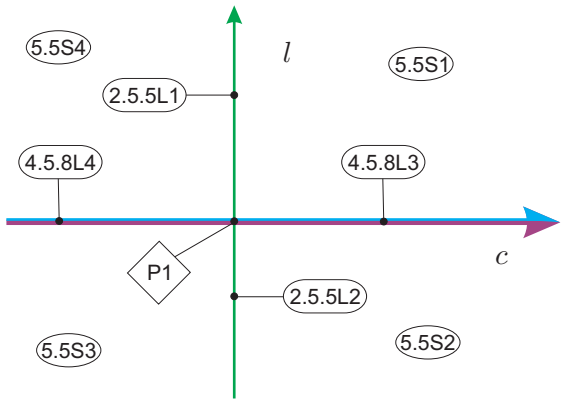

Fig. 9. Plane $m = 0$ on the slice $n = 0$ (see Fig. 8)

$m = 0$, which indicate, respectively, the generic and the singular planes.

For the values of the parameters d and n under consideration, we have that $(\mathcal{V}_8)$ is reduced to the double line $c^2 = 0$. Therefore, for $m = 1$, this is the only topological change in the bifurcation diagram when we compare this plane with the plane described in Fig. 6 (see Fig. 10).

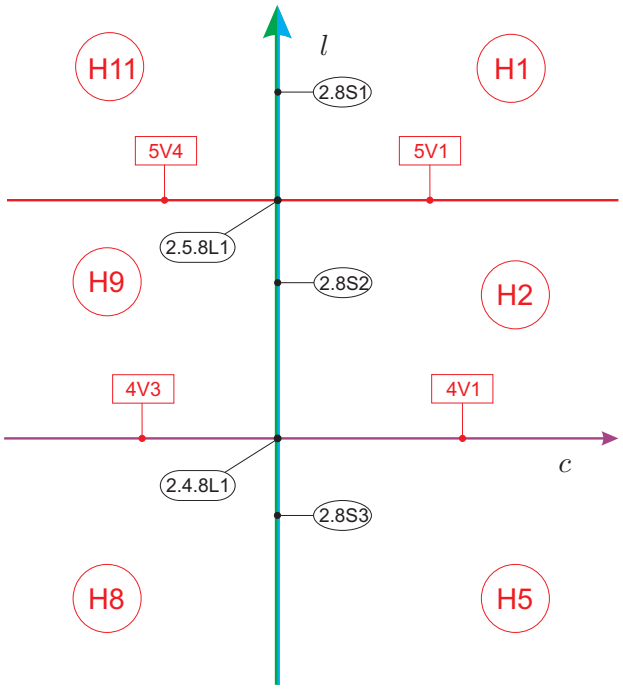

Fig. 10. Plane $m = 1$ on the affine part of the infinity of $\mathbb{RP}^4$ (see Fig. 9)

Using the same arguments as before, we conclude that in the plane $m = 0$ we have only one topological change on the bifurcation diagram when we compare this plane with the plane described in Fig. 7 (see Fig. 11).

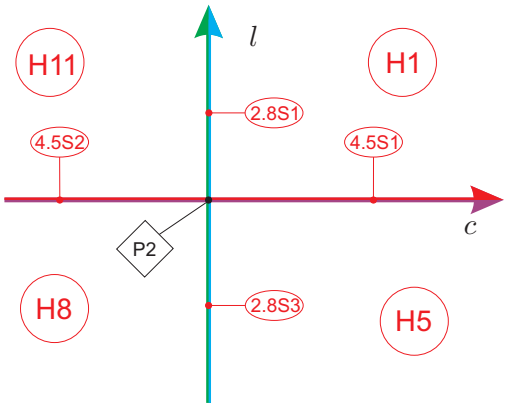

Fig. 11. Plane $m = 0$ on the affine part of the infinity of $\mathbb{RP}^4$ (see Fig. 10)

Remark 6.1. The phase portrait corresponding to region $2.8S_1$ in Fig. 10 possesses a pair of complex straight lines filled up with singularities. Such straight lines are described by equations

$$y = (-1 \pm i)x,$$

respectively. We point out that this phase portrait is topologically equivalent to $2V_1$ from Fig. 2. This is a very curious topological coincidence of phase portraits coming from very different quadratic systems. There is even one more quadratic system topologically equivalent to them but geometrically different, which is the one that has the intricate point $hh_{(4)}$. This fact has already been detected in different papers as [Artés & Libre, 1994] or [Artés *et al.*, 2020b].

Now, finally we present the study of the infinity of the infinite part of $\mathbb{RP}^4$. Here we already have $d = n = 0$, i.e. we are in the half–sphere $c^2 + l^2 + m^2 = 1$. Then we proceed as we did in the previous section, that is, here we have to study $m = 1$ (the affine part) and $m = 0$ (the equator). For these values of d and n we have that $(\mathcal{V}_5) \equiv 0$ and $(\mathcal{V}_8) \equiv 0$, then all the phase portraits that will be obtained here are degenerate. Moreover, equation (8) tells us that the vertical axis is still a bifurcation curve because on it the degeneration is of degree two. But we verify that the horizontal axis still

produces an invariant straight line but now does not imply any topological change on the bifurcation diagram, this is the reason why we have drawn this axis as a dashed line in Fig. 12. In such a figure, all the "generic" parts are labeled as $8.9S_j$, the lines are labeled as $k.8.9L_j$, where k corresponds to the curve on this compactified plane, and the points are labeled as points. We use the orange color for the equator of $\mathbb{S}^2$, i.e. $d = n = m = 0$.

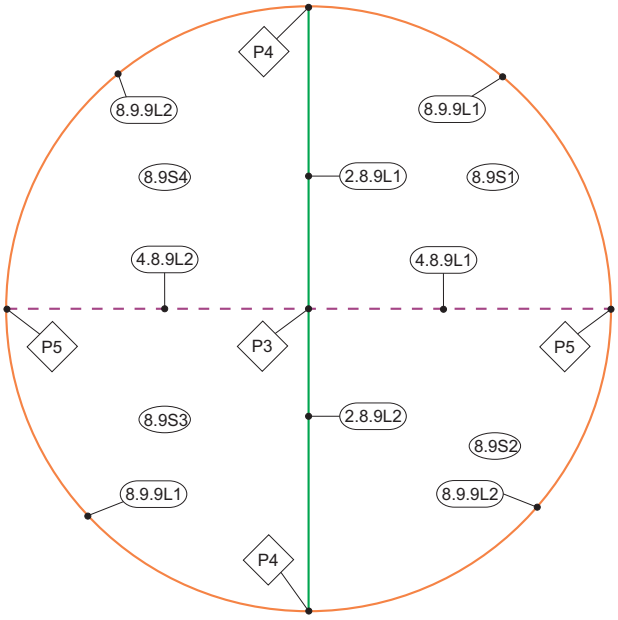

Fig. 12. Compactified plane corresponding to the infinite part of the infinity of $\mathbb{RP}^4$. The affine part is given by $n = 0, m = 1$ and the equator is described by $n = m = 0$ (see Fig. 11)

Since the complete bifurcation diagram is quite simple, the best way to see the continuity between different phase portraits, and the way that they bifurcate ones from the others, is to set all the planes in a single page in a reduced size as we do in Fig. 13.

Because there is coherence among all the slices that we have presented, we conclude that no more slices are needed for the complete coherence of the bifurcation diagram and therefore we can affirm that we have described a complete bifurcation diagram for family $\overline{\mathbf{QsnSN_{11}(A)}}$ modulo islands, as discussed in Sec. 7.

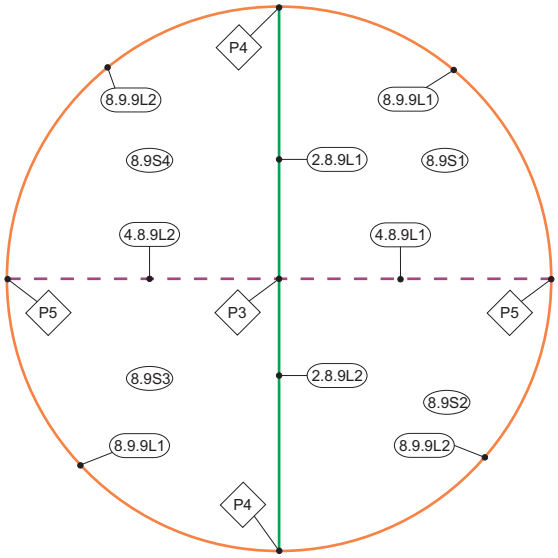

$d = 0, n = 0, m = 1$ (affine)
$d = 0, n = 0, m = 0$ (equator)

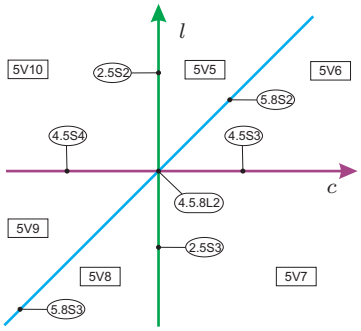

$d = 1, n = 0, m = 1$

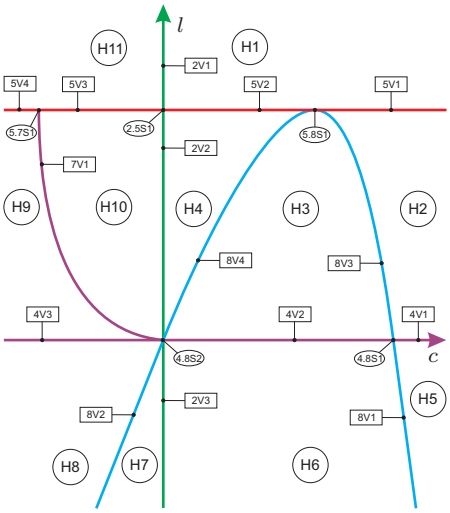

$d = 1, n = 1, m = 1$

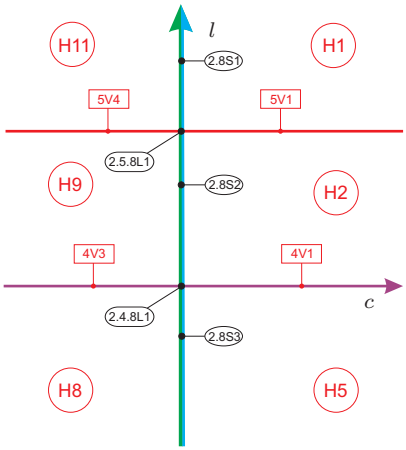

$d = 0, n = 1, m = 1$

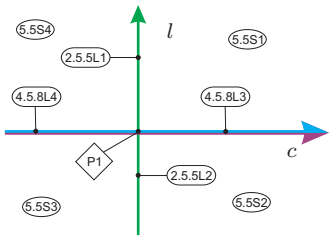

$d = 1, n = 0, m = 0$

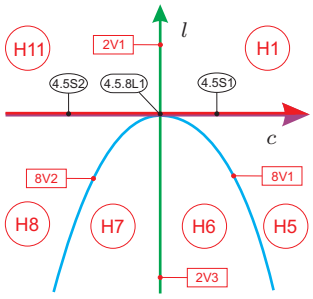

$d = 1, n = 1, m = 0$

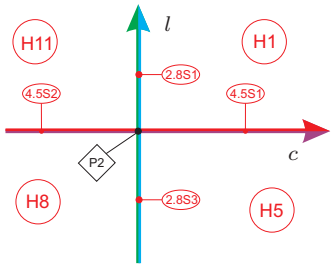

$d = 0, n = 1, m = 0$

Fig. 13. All cl–planes of the bifurcation diagram and the corresponding values of the parameters d, m and n

7. Other relevant facts about the bifurcation diagram

The bifurcation diagram that we have obtained for the class $\overline{\mathbf{QsnSN_{11}(A)}}$ is completely coherent, i.e. in each plane, by taking any two points in the parameter space and joining them by a continuous curve, along this curve the changes in phase portraits that occur when crossing the different bifurcation surfaces we mention can be completely explained.

Nevertheless, we cannot be sure that these bifurcation diagram is the complete bifurcation diagram for $\overline{\mathbf{QsnSN_{11}(A)}}$ due to the possibility of "islands" inside the parts bordered by unmentioned bifurcation manifolds. In case they exist, these "islands" would not mean any modification of the nature of the singular points.

In case there were more bifurcation manifolds, we should still be able to join two representatives of any two parts of the 75 parts of $\overline{\mathbf{QsnSN_{11}(A)}}$ found until now with a continuous curve either without crossing such a bifurcation manifold or, in case the curve crosses it, it must do it an even number of times without tangencies, otherwise one must take into account the multiplicity of the tangency, so the total number must be even. This is why along this text we call these potential bifurcation manifolds "*islands*". In order to be more precise, we have to answer the following question: What such a phase portrait could be in such an island? If we consider the phase portraits from [Artés *et al.*, 2018] and from those ones of family (A) of codimension–one (which possess a finite saddle–node $\overline{sn}_{(2)}$, see page 3) and forcing the coalescence of two finite singular points with two different infinite singular points to produce a phase portrait of $\overline{\mathbf{QsnSN_{11}(A)}}$, we can detect up to eight different phase portraits, in such a way that two of them do not appear here. Under some conditions these phase portraits could live in such an island inside the bifurcation diagram. However, using other arguments, it can be proved that they are not realizable. We delay the proof of this fact since this will be the main matter on a future paper on the topological classification of all the phase portraits of the class $\mathbf{QsnSN_{11}}$.

8. Completion of the proof of the main theorem

In the bifurcation diagram we may have topologically equivalent phase portraits belonging to distinct parts of the parameter space. As here we have 75 distinct parts of the parameter space, to help us identify or distinguish phase portraits, we need to introduce some invariants and we actually choose integer valued, character and symbol invariants. Some of them were already used for instance in [Artés *et al.*, 2015], but we recall them and introduce some needed ones. These invariants yield a classification which is easier to grasp.

First of all we would like to emphasize that due to some values of the parameters, among the 75 phase portraits obtained in the study of the bifurcation diagram, four of them correspond to linear systems (see page 22). These four phase portraits can be clearly divided into two classes as in Fig. 1 (we can distinguish them by considering, for instance, the number of infinite singularities, which is a numeric invariant).

Now we define six invariants I_j, $1 \leq j \leq 6$, that allows us to make the classification of the remaining 71 phase portraits corresponding to quadratic differential systems.

Definition 8.1. We denote by $I_1(S)$ the number of the real finite singular points. We note that this number can also be infinity, which is represented by ∞.

Definition 8.2. We denote by $I_2(S)$ the number of the real infinite singular points.

Definition 8.3. For a given infinite singularity s of a system S, let ℓ_s be the number of global or local separatrices beginning or ending at s and which do not lie on the line at infinity. Then $0 \leq \ell_s \leq 4$. We denote by $I_3(S)$ the sequence of all such ℓ_s when s moves in the set of infinite singular points of system S. We start the sequence at the infinite singular point which receives (or sends) the greatest number of separatrices and take the direction which yields the greatest absolute value, e.g. the values 2110 and 2011 for this invariant are symmetrical (and, therefore, they are the same), so we consider 2110.

Definition 8.4. We denote by $I_4(S)$ the total

number of local or global separatrices of the finite multiple singular point linking it to the infinite multiple singular points.

Definition 8.5. We denote by $I_5(S)$ a character from the set {n,y} describing the nonexistence ("n") or the existence ("y") of elliptic sectors.

Definition 8.6. We denote by $I_6(S)$ a symbol from the set $\{[|], [|_2], [\times]\}$ which indicates the following configuration of curves filled up with singularities, respectively: a real straight line, a double real straight line, and two real straight lines intersecting at a finite point. This invariant only makes sense to distinguish the degenerate phase portraits.

Theorem 8.7. *Consider the class* $\overline{\mathbf{QsnSN_{11}(A)}}$ *and all the phase portraits that we have obtained for this family. The values of the affine invariant* $\mathcal{I} = (I_1, I_2, I_3, I_4, I_5, I_6)$ *given in Table 8.1 yield a partition of these phase portraits of the class* $\overline{\mathbf{QsnSN_{11}(A)}}$.

Furthermore, for each value of $\mathcal{I}$ *in this diagram there corresponds a single phase portrait; i.e.* S *and* S' *are such that* $\mathcal{I}(S) = \mathcal{I}(S')$*, if and only if* S *and* S' *are topologically equivalent.*

The bifurcation diagram for $\overline{\mathbf{QsnSN_{11}(A)}}$ has four parts corresponding to two topologically distinct classes of linear systems and also 71 parts corresponding to quadratic ones. As we have said before, the phase portraits corresponding to linear systems can be easily divided into two different classes, as in Fig. 1. Now we have to work in the classification of the remaining 71 parts. These ones produce 34 topologically different phase portraits as described in Table 8.2 and the remaining 37 parts do not produce any new phase portrait.

The phase portraits that does not possess graphic have been denoted surrounded by parenthesis, for example $(5V_2)$; the phase portraits having two or more graphics have been denoted surrounded by $\{\{*\}\}$, for example $\{\{P_4\}\}$. Normally we use a single $\{*\}$ when there is just one graphic but this does not happen in the present study.

Proof of Theorem 8.7. The above result follows from the results in the previous sections and a careful analysis of the bifurcation planes given in Sec. 4, in Figs. 4 to 12, the definition of the invariants I_j and their explicit values for the corresponding phase portraits. ■

Regarding the phase portraits corresponding to quadratic systems, in Table 8.2 we list in the first column 34 parts with all the distinct phase portraits of Fig. 2. Corresponding to each part listed in the first column we have in each row all parts whose phase portraits are topologically equivalent to the phase portrait appearing in the first column of the same row.

In the second column we set all the parts whose systems yield topologically equivalent phase portraits to those in the first column, but which are identical under perturbations.

In the third column we list all parts whose phase portraits possess an invariant curve not yielding a connection of separatrices.

In the fourth column we add the phase portraits, topologically equivalent to those ones from the first column, which corresponds to symmetric parts of the bifurcation diagram.

The last column refers to other reasons associated to different geometrical aspects and they are described as follows:

(1) the phase portrait possesses a singularity of type $\widehat{\binom{2}{3}}PP - PP$ at infinity;
(2) the coincidence described in Remark 6.1.

Whenever phase portraits appear in a row in a specific column, the listing is done according to the decreasing dimension of the parts where they appear, always placing the lower dimensions on lower rows.

Regarding the linear differential systems obtained in this study which correspond to the parts $4.5.8L_3, 4.5.8L_4, P_1, P_5$ of the bifurcation diagram (see Figs. 9 and 11), as we have mentioned before, we can split them into two different classes as in Fig. 1. By considering, for instance, the number of infinite singularities we obtain that $4.5.8L_3, 4.5.8L_4, P_5$ have two distinct infinite singularities whereas P_1 has only one infinite singularity. Therefore we conclude the classification of all phase portraits obtained by the study of the class $\overline{\mathbf{QsnSN_{11}(A)}}$ with respect to the canonical form (6).

Table 8.1. Geometric classification for the family $\mathbf{QsnSN_{11}}(\mathbf{A})$

$$
I_1 = \begin{cases}
1 \;\&\; I_2 = \begin{cases}
1 \;\&\; I_3 = \begin{cases} 11\ (2V_1), \\ 21\ (H_1), \end{cases} \\
2 \;\&\; I_3 = \begin{cases}
1110 \;\&\; I_4 = \begin{cases} 2\ (4.5S_1), \\ 3\ \{\{4.5S_3\}\}, \end{cases} \\
2100\ (5.7S_1), \\
2101 \;\&\; I_4 = \begin{cases} 1\ (5V_1), \\ 2\ \{\{2.5S_2\}\}, \\ 3\ \{\{5V_6\}\}, \end{cases} \\
2200\ (2.5S_1), \\
2210\ \{\{5V_7\}\}, \\
3101\ \{\{5V_5\}\}, \\
3200 \;\&\; I_4 = \begin{cases} 1\ (5V_2), \\ 2\ (5V_3), \end{cases}
\end{cases} \\
3 \;\&\; I_3 = \begin{cases}
111010\ (4V_1), \\
111110\ (H_5), \\
210110\ (4V_2), \\
211010\ (7V_1), \\
211110 \;\&\; I_4 = \begin{cases} 1\ (H_2), \\ 2\ (H_3), \end{cases} \\
220110\ (2V_3), \\
311010\ (2V_2), \\
320110\ (H_6), \\
321010\ (H_{10}), \\
411010\ (H_4),
\end{cases}
\end{cases} \\
\infty \;\&\; I_2 = \begin{cases}
1 \;\&\; I_5 = \begin{cases} \text{n}\ \{\{P_4\}\}, \\ \text{y}\ \{\{8.9.9L_1\}\}, \end{cases} \\
2 \;\&\; I_3 = \begin{cases}
0000 \;\&\; I_5 = \begin{cases}
\text{n} \;\&\; I_6 = \begin{cases} []\ (4.5.8L_1), \\ [|_2]\ (2.5.8L_1), \\ [\times]\ \{\{2.8.9L_1\}\}, \end{cases} \\
\text{y}\ \{\{5.8S_2\}\},
\end{cases} \\
1000\ \{\{8.9S_1\}\}, \\
1010\ \{\{5.8S_1\}\},
\end{cases} \\
3 \;\&\; I_3 = \begin{cases} 000000\ \{\{2.8S_2\}\}, \\ 100000\ \{\{8V_1\}\}. \end{cases}
\end{cases}
\end{cases}
$$

Table 8.2. Topological equivalences for the family $\mathbf{QsnSN_{11}(A)}$

Presented phase portrait	Identical under perturbations	Possessing invariant curve (no separatrix)	Symmetry	Other reasons
H_1	H_{11}			$5.5S_1{}^{(1)}$, $5.5S_2{}^{(1)}$, $5.5S_3{}^{(1)}$, $5.5S_4{}^{(1)}$
H_2	H_9			
H_3				
H_4				
H_5	H_8			
H_6	H_7			
H_{10}				
$2V_1$				$2.8S_1{}^{(2)}$ $2.5.5L_1{}^{(1)}$, $2.5.5L_2{}^{(1)}$
$2V_2$				
$2V_3$				
$4V_1$	$4V_3$			
$4V_2$				
$5V_1$	$5V_4$			
$5V_2$				
$5V_3$				
$5V_5$			$5V_8$	
$5V_6$			$5V_9$	
$5V_7$			$5V_{10}$	
$7V_1$				
$8V_1$	$8V_2$, $8V_3$, $8V_4$	$4.8S_1$, $4.8S_2$		
$2.5S_1$				
$2.5S_2$			$2.5S_3$	
$2.8S_2$	$2.8S_3$	$2.4.8L_1$		
$4.5S_1$			$4.5S_2$	
$4.5S_3$			$4.5S_4$	
$5.7S_1$				
$5.8S_1$				
$5.8S_2$		$4.5.8L_2$	$5.8S_3$	
$8.9S_1$		$4.8.9L_1$, $4.8.9L_2$	$8.9S_2$, $8.9S_3$, $8.9S_4$	
$2.5.8L_1$	P_2			
$2.8.9L_1$		P_3	$2.8.9L_2$	
$4.5.8L_1$				
$8.9.9L_1$			$8.9.9L_2$	
P_4				

Acknowledgements. The first author is partially supported by a MEC/FEDER grant number MTM 2016–77278–P and by a CICYT grant number 2017 SGR 1617. This study was financed in part by the Coordenação de Aperfeiçoamento de Pessoal de Nivel Superior - Brazil (CAPES) - Finance Code 001 (the second author is partially supported by this grant). The third author is partially supported by CAPES and by FAPESP Processo no. 2018/21320-7.

References

Artés, J.C., Dumortier, F., Herssens, C., Llibre, J. & de Maesschalck, P. [2005] "Computer program P4 to study phase portraits of planar polynomial differential equations," Available at: <`http://mat.uab.es/~artes/p4/p4.htm`>.

Artés, J.C., Kooij, R. & Llibre, J. [1998] "Structurally stable quadratic vector fields," *Memoires Amer. Math. Soc.* **134 (639)**, 108pp.

Artés & J.C., Llibre, J. [1994] "Quadratic Hamiltonian vector fields," *J. Differential Equations* **107**, 80–95.

Artés, J.C., Llibre, J. & Rezende, A.C. [2018] "Structurally unstable quadratic vector fields of codimension one." 1. ed. *Birkhäuser*. v.1. 267p.

Artés, J.C., Llibre, J. & Schlomiuk, D. [2006] "The geometry of quadratic differential systems with a weak focus of second order," *Internat. J. Bifur. Chaos Appl. Sci. Engrg.* **16**, 3127–3194.

Artés, J.C., Llibre, J. & Vulpe, N. [2008] "Singular points of quadratic systems: a complete classification in the coefficient space $\mathbb{R}^{12}$," *Internat. J. Bifur. Chaos Appl. Sci. Engrg.* **18**, 313–362.

Artés, J.C., Llibre, J., Schlomiuk, D. & Vulpe, N. [2013a] "Geometric configurations of singularities for quadratic differential systems with total finite multiplicity lower than 2," *Bul. Acad. Ştiinţe Repub. Mold. Mat.* **71**, 72–124.

Artés, J.C., Llibre, J., Schlomiuk, D. & Vulpe, N. [2020a] "Geometric configurations of singularities of planar polynomial differential systems - A global classification in the quadratic case". To be published by Birkhäuser.

Artés, J.C., Llibre, J., Schlomiuk, D. & Vulpe, N. [2020b] "Global topological configurations of singularities for the whole family of quadratic differential systems," *Qualitative Theory on Dynamical Systems* **19**, (51), 32pp.

Artés, J.C., Oliveira, R.D.S. & Rezende, A.C. [2019] "Structurally unstable quadratic vector fields of codimension two: families possessing either a cusp point or two finite saddle–nodes," *preprint* , 48pp.

Artés, J.C., Rezende, A.C. & Oliveira, R.D.S. [2013b] "Global phase portraits of quadratic polynomial differential systems with a semi–elemental triple node," *Internat. J. Bifur. Chaos Appl. Sci. Engrg.* **23**, 21pp.

Artés, J.C., Rezende, A.C. & Oliveira, R.D.S. [2014] "The geometry of quadratic polynomial differential systems with a finite and an infinite saddle–node (A, B)," *Internat. J. Bifur. Chaos Appl. Sci. Engrg.* **24**, 30pp.

Artés, J.C., Rezende, A.C. & Oliveira, R.D.S. [2015] "The geometry of quadratic polynomial differential systems with a finite and an infinite saddle–node C.," *Internat. J. Bifur. Chaos Appl. Sci. Engrg.* **25**, 111pp.

Bautin, N.N. [1954] "On periodic solutions of a system of differential equations," *Prikl. Mat. Meh.* **18**, 128.

Coll, B., Gasull, A. & Llibre, J. [1988a] "Quadratic systems with a unique finite rest point," *Publ. Mat.* **32**, 199–259.

Coll, B. & Llibre, J. [1988b] "Limit cycles for a quadratic system with an invariant straight line and some evolution of phase portraits," *Qualitative Theory of Differential Equations, Colloq. Math. Soc. János Bolyai, Bolyai Institut, Szeged, Hungria* **53**, 111–123.

Coppel, W.A. [1966] "A survey of quadratic systems," *J. Differential Equations* **2**, 293–304.

Dumortier, F., Llibre, J. & Artés, J.C. [2006] "Qualitative Theory of Planar Differential Systems," *Universitext, Springer–Verlag, New York–Berlin.*

Dumortier, F., Roussarie, R. & Rousseau, C. [1994] "Hilbert's 16th problem for quadratic vector fields," *J. Differential Equations* **110**, 66–133.

Hilbert, D. [1900] "Mathematische probleme", *In Nachr. Ges. Wiss., editor Second Internat. Congress Math. Paris, 1900*, 253–297. Göttingen Math.–Phys. Kl.

Hilbert, D. [1902] "Mathematical problems," *Bull. Amer. Math. Soc.* **8**, 437–479.

Jager, P. [1990] "Phase portraits for quadratics systems with a higher order singularity with two zero eigenvalues," *J. Diff. Eqns.* **87**, 169–204.

Schlomiuk, D. & Vulpe, N.I. [2004] "Planar quadratic vector fields with invariant lines of total multiplicity at least five," *Qualitative Theory of Dynamical Systems* **5**, 135–194.

Schlomiuk, D. & Vulpe, N.I. [2005] "Geometry of quadratic differential systems in the neighborhood of the infinity," *J. Differential Equations* **215**, 357–400.

Vulpe, N.I. [2011] "Characterization of the finite weak singularities of quadratic systems via invariant theory," *Nonlinear Anal.* **74**, 6553–6582.

Zhang, P. [2001] "Quadratic systems with a 3rd–order (or 2nd–order) weak focus," *Ann. Differential Equations* **17**, 287–294.